
Tumor Pretargeting in Mice Using ^{99m}Tc -Labeled Morpholino, a DNA Analog

Guozheng Liu, PhD; Kennedy Mang'era, PhD; Ning Liu, MD; Suresh Gupta, PhD; Mary Rusckowski, PhD; and Donald J. Hnatowich, PhD

Division of Nuclear Medicine, Department of Radiology, University of Massachusetts Medical School, Worcester, Massachusetts

Over the past several years, investigators in this laboratory and elsewhere have been studying tumor localization by pretargeting with streptavidin and biotin or with avidin and biotin. Despite encouraging results, difficulties related to endogenous biotin and the immunogenicities of streptavidin and avidin have made a search for alternative strategies sensible. Recently, we have considered the use of DNAs and peptide nucleic acids for this purpose because oligomers can have hybridization affinities equivalent to that of biotin for streptavidin or avidin without the associated difficulties. We now report on the use of a morpholino (MORF), another commercially available synthetic oligomer, for pretargeting applications. MORFs support the nitrogenous bases by nonionic phosphorodiamidate linkages and, besides being nuclease resistant, can display good water solubility. **Methods:** An 18mer MORF and its 18mer complementary MORF (cMORF) were obtained with a primary amine through a 3-member alkyl linker on the 3' equivalent end. An anti-carcinoembryonic antigen IgG antibody (MN14) was conjugated with MORF, whereas cMORF was conjugated with *N*-hydroxysuccinimide-mercaptopropylglycine (MAG3) to permit radiolabeling with ^{99m}Tc . The biodistribution of labeled cMORF was first evaluated in normal CD-1 mice. Subsequently, nude mice bearing LS174T tumors received 50 μg conjugated antibody 48 h before the administration of 1.0 μg (7.4 MBq) ^{99m}Tc -MAG3-cMORF. Control animals received the labeled cMORF without prior administration of the antibody. A clearing step was not used. **Results:** Biodistributions in normal mice showed that ^{99m}Tc -MAG3-cMORF was excreted rapidly through the kidneys, with only 7 percentage injected dose (%ID) remaining within the whole body (excluding urine) at 3 h. In tumor-bearing mice at 24 h, only 11 %ID of the radioactivity remained in the whole body of study animals, and of this amount, 2 %ID/g was in tumor tissue. The sites with the highest %ID were the kidneys, at 4 %ID/g, and the blood, at 0.5 %ID/g; all other organs had <1 %ID/g. At the same time, values for the control animals were 5 %ID (whole body), 0.05 %ID/g (tumor), and 3 %ID (kidneys). All images reflected high uptake in the tumors and low uptake in the normal tissues of the study mice. **Conclusion:** Pretargeting using MORFs was effective in a mouse tumor model.

Key Words: antibody; pretargeting; ^{99m}Tc ; oligomer

J Nucl Med 2002; 43:384–391

Received Jun. 1, 2001; revision accepted Nov. 12, 2001.
For correspondence or reprints contact: Donald J. Hnatowich, PhD, Division of Nuclear Medicine, Department of Radiology, University of Massachusetts Medical School, 55 Lake Ave. North, Worcester, MA 01655-0243.
E-mail: Donald.hnatowich@umassmed.edu

The use of radiolabeled antibodies in nuclear medicine to target tumors was first investigated in the 1970s (1) and has since been studied extensively. However, the limitations of conventional tumor imaging have long been recognized and include prolonged targeting time and slow clearance from background tissues. Subsequent approaches have been pursued that seek to bring about faster tumor targeting and excretion by use of smaller antibody fragments or small peptides as substitutes for the whole antibody (2–4). Background radioactivity levels have been improved in this manner, and use of the smaller radiolabeled antitumor agents has improved penetrability into tumors. Nevertheless, further improvements in tumor uptake and in ratios of tumor to normal tissue would be welcome.

One alternative approach to conventional tumor imaging is pretargeting. Several review articles on this topic have appeared (5–10). Pretargeting involves the administration of a nonradioactive tumor-specific agent carrying a molecular group with a high affinity for a small effector molecule. After a suitable interval to allow for tumor targeting and clearance, the radiolabeled effector is administered. Thus, the pretargeting method allows for clearance of the tumor-specific antibody from normal tissues before administration of the radiolabeled effector and therefore can potentially overcome the intrinsic disadvantage of the lower ratios of tumor radioactivity to normal tissue radioactivity that are characteristic of conventional targeting. Ideally, the effector should be a small hydrophilic, nonimmunogenic, highly diffusible molecule that is rapidly and principally excreted by the kidneys. At least 3 recognition systems have been reported: streptavidin (or avidin) and biotin (11), bispecific antibody and hapten (12), and DNA and complementary DNA (13).

The system that uses streptavidin (or avidin) and biotin has been the most extensively studied, and impressive results have been reported (14–16). Avidin is a protein of approximately 66 kDa, existing in egg white, and streptavidin is a similarly large protein of approximately 60 kDa, isolated from bacteria. Biotin is a 244-Da essential vitamin that exists in blood and tissues in low concentrations and has a high affinity (dissociation constant, approximately 10^{-15} mol/L) for streptavidin and avidin. The drawbacks of

this system include potential instability of the radiolabeled biotin to plasma biotinidase degradation (9,17) and immunogenicity of streptavidin and avidin, especially when conjugated to antibody (18). More troubling to this approach can be the influence of endogenous biotin, which can compete effectively with radiolabeled biotin for the streptavidin and avidin sites (19,20). A 3-step strategy involving administration of biotinylated monoclonal antibody, avidin, and then radiolabeled biotin alleviates some of the drawbacks, but this procedure is considered complex for imaging and does not address immunogenicity.

The second recognition system uses a radiolabeled hapten and a bispecific antibody in place of streptavidin (or avidin) and biotin (10,21–24). The hapten often is a coordination complex, for example, indium-diethylenetriaminepentaacetic acid. The bispecific antibody is the product of linking 2 antibodies or antibody fragments against separate determinants, the hapten and a tumor marker such as carcinoembryonic antigen. In addition to requiring the preparation of bispecific antibodies, this approach may suffer from lower affinities. The affinity of an antibody for its hapten, particularly for a monovalent one, is orders of magnitude lower than that of streptavidin or avidin for biotin. Mathematic modeling has shown that a high affinity between an antibody and its hapten is an important determinant of successful pretargeting (25).

The recognition system that uses an oligomer and a complementary oligomer has been comparatively less investigated (13,26,27). The suitability of the native phosphodiester DNA as an effector is compromised by its susceptibility to nuclease hydrolysis. Several chemical analogs of single-stranded DNA have been developed with variations at the phosphodiester backbone, principally to improve the in vivo stability of the native form. Although the phosphorothioate DNA oligomer is stable to nucleases, its principal disadvantage is its affinity for tissue and plasma proteins (28). One synthetic DNA analog, peptide nucleic acid (PNA), is excreted rapidly, is stable, and seems to meet the requirements of an effector for pretargeting. A 15mer PNA was previously evaluated in this laboratory for pretargeting (26). Morpholino oligomers (MORFs), like PNA, are synthetic DNA analogs that have recently become commercially available and are reported to be water soluble, stable to nucleases, and highly specific for its complementary MORF (29). Preliminary results from this laboratory have shown that a radiolabeled MORF can hybridize in vivo with its complementary sequence (30).

This laboratory has investigated labeled DNAs and PNAs for pretargeting (26,31). We now report on the coupling of an 18mer MORF to a tumor-specific anti-carcinoembryonic antigen (CEA) IgG antibody (MN14) and its use in pretargeting studies of LS174T tumor-bearing mice with ^{99m}Tc -labeled 18mer complementary MORF (cMORF).

MATERIALS AND METHODS

A 3'-amine-derivatized 18mer MORF (molecular weight, 6,156 Da), a biotinylated 18mer MORF, an 18mer 3'-amine-derivatized cMORF (molecular weight, 6,107 Da), and a biotinylated 18mer cMORF were gifts from GeneTools, LLC (Philomath, OR). The amine and biotin moieties were conjugated through a 3-carbon β -alanine linker on the 3'-equivalent end. The base sequences of MORF and cMORF were 5'-GGGTGTACGTCAACAATA and 5'-TAGTTGTGACGTACACCC, respectively. Streptavidin-coated magnetic beads (BioMag Streptavidin Ultra-Load) were purchased from Polysciences, Inc. (Warrington, PA). A high-affinity murine anti-CEA antibody (MN14; IgG 1 subtype; molecular weight, 150 kDa) was a gift of Immunomedics (Morris Plains, NJ). 1-Ethyl-3-(3-dimethylaminopropyl)-carbodiimide hydrochloride (EDC) was purchased from Pierce Chemical Co. (Rockford, IL). *S*-acetyl *N*-hydroxysuccinimide (NHS)-mercaptoacetyltriglycine (MAG3) was synthesized in house (32), and its structure confirmed by elemental analysis, proton nuclear magnetic resonance, and mass spectroscopy. Bio-Gel P4 medium for separation was purchased from Bio-Rad Laboratories Inc. (Hercules, CA), and Sephadex G-100 was purchased from Amersham Pharmacia Biotech (Piscataway, NJ). ^{99m}Tc -pertechnetate was eluted from a $^{99\text{m}}\text{Mo}$ - ^{99m}Tc generator (DuPont Pharmaceuticals Co., Billerica, MA). All other chemicals were reagent grade and were used without further purification.

HPLC Methods

Size-exclusion (SE) high-performance liquid chromatography (HPLC) was performed on a Superose 12 column (HR10/30; Amersham Pharmacia Biotech) with 0.10 mol/L phosphate buffer, pH 7.0, as eluent at a flow rate of 0.6 mL/min. In-line ultraviolet absorbance and radioactivity detectors were used to detect and quantitate peak fractions. Recovery of radioactivity was determined routinely.

Preparation of cMORF-MAG3

An amount of *S*-acetyl NHS-MAG3 was added to a 3.5 $\mu\text{g}/\mu\text{L}$ solution of cMORF in 0.2 mol/L *N*-(2-hydroxyethyl)piperazine-*N'*-(2-ethanesulfonic acid) buffer, pH 8.0, and after the sample was stirred, the mixture was incubated at room temperature for at least 1 h. The molar ratio of cMORF to *S*-acetyl NHS-MAG3 was approximately 1:20. The solution was purified on a 0.7 \times 20 cm P4 column with 0.25 mol/L ammonium acetate buffer, pH 5.2. The concentration with respect to cMORF of the recovered fraction was estimated by ultraviolet absorbance at 265 nm using an absorbance coefficient of 31 $\mu\text{L}/\mu\text{g}$ for cMORF. The purified MAG3-cMORF solution was stored at -20°C .

Labeling of cMORF-MAG3 with ^{99m}Tc

To 25 μL MAG3-cMORF in 0.25 mol/L, pH 5.2, ammonium acetate solution ($>0.1 \mu\text{g}/\mu\text{L}$ cMORF) were added 6 μL sodium tartrate solution (50 $\mu\text{g}/\mu\text{L}$, pH 9.2) and 2 μL stannous chloride dihydrate solution in 10 mmol/L HCl (1 $\mu\text{g}/\mu\text{L}$), followed immediately by 3.7–37 MBq (2–30 μL) ^{99m}Tc -pertechnetate generator eluent. The final pH was approximately 7.6. The solution was heated in a boiling water bath for 20 min before the labeling mixture was purified on a 0.7 \times 20 cm P4 column using 0.05 mol/L phosphate buffer, pH 7.0. Labeling efficiency was calculated as the percentage of radioactivity recovered in the cMORF peak. Preparations of radiolabeled cMORF were analyzed further by SE HPLC.

Preparation of MN14-MORF

An aliquot of MN14 solution (100 μL of 10 $\mu\text{g}/\mu\text{L}$ in 0.04 mol/L phosphate buffer saline, pH 7) was mixed with MORF (250 μL of a 2.4 $\mu\text{g}/\mu\text{L}$ solution in 0.1 mol/L 2-[N-morpholino]ethanesulfonic acid buffer, pH 5.0). EDC (1 mg, 20 $\mu\text{g}/\mu\text{L}$) in the latter buffer was then immediately added. The molar ratios of MN14:MORF:EDC were 1:15:750. The reaction mixture was incubated at room temperature for at least 1 h. Purification was achieved on a 0.7×20 cm Sephadex G-100 column with 0.05 mol/L, pH 7.0, phosphate buffer as eluent. The concentration of the recovered fraction was estimated with respect to MN14 by ultraviolet absorbance at 280 nm using an absorbance coefficient of 1.40 $\mu\text{L}/\mu\text{g}$. The purified solution was stored at -20°C .

Hybridization Ability of $^{99\text{m}}\text{Tc}$ -Labeled cMORF

Binding to beads is a convenient method to evaluate hybridization between an oligomer and its complement (31,33). After optimization of hybridization conditions, the hybridization ability of radiolabeled cMORF was evaluated on streptavidin-coated magnetic beads.

The beads (300 μL) were washed 3 times with 200 μL washing buffer (20 mmol/L Tris buffer and 0.5 mol/L sodium chloride, pH 8.2), while retained in the tube using a magnetic separator (MPC; Dynal Biotech, Inc., Lake Success, NY). After the last wash, the beads were suspended in 200 μL washing buffer, 1.0 μg biotin-MORF was added, and 15 min later, the beads were again washed 3 times with 200 μL washing buffer. After resuspension in 200 μL washing buffer, 2 μL radiolabeled MORF (0.02 μg cMORF) were added. After 1 h of incubation with constant agitation, the beads were separated, washed 3 times, and counted in a NaI(Tl) well counter. The supernatant and washing solutions were combined and counted. Two control groups of beads, one without biotin-MORF and one with biotin-cMORF substituted for biotin-MORF, were simultaneously carried through the identical procedure.

Estimation of MORF Groups per Molecule on Coupled MN14

After coupling, the MORF on MN14 could not be quantitated by its ultraviolet absorbance. To estimate the number of MORF groups on MN14, a series of aliquots of purified radiolabeled cMORF (4, 25, 50, and 150 μL at 0.01 $\mu\text{g}/\mu\text{L}$) was added to 50 μL MN14-MORF (0.5 $\mu\text{g}/\mu\text{L}$), incubated at room temperature for 1 h, and analyzed by SE HPLC. A control study was performed identically with 4 μL (0.01 $\mu\text{g}/\mu\text{L}$) radiolabeled cMORF but added to native MN14. Using SE HPLC, radioactivity bound to MN14 was detected by the shift in radioactivity profile to a higher molecular weight (earlier retention time) from labeled cMORF to labeled cMORF-MN14-MORF.

Biodistribution of Labeled cMORF in Normal CD-1 Mice

Each of 12 normal CD-1 mice (body weight range, 30–35 g) received 1.5 μg (3.7 MBq) labeled cMORF by tail vein injection. Four mice were killed at each of 3 intervals: 0.5, 1, and 3 h. The mice were dissected, urine was carefully drawn, and organs were removed and weighed. The radioactivity in each organ was counted in the NaI(Tl) well counter along with blood samples of known volume and an aliquot of the injectate. The radioactivity remaining in the carcass was measured in a dose calibrator.

Pretargeting of Labeled cMORF in LS174T Tumor-Bearing Nude Mice

Each of 8 nude mice (body weight range, 25–30 g) received 10^6 LS174T colon tumor cells by injection in 0.1 mL into 1 thigh. After 12 d, when the tumors were no more than 1 cm in any dimension, 4 of the animals received 50 μg MN14-MORF. After 48 h, 1.0 μg labeled cMORF (7.4–8.9 MBq) was injected through a tail vein into both the mice that had and the mice that had not received the MN14-MORF. At 3 and 24 h after injection of the labeled cMORF, the animals were anesthetized with ketamine plus xylazine and imaged anteriorly with a scintillation camera (Elscont, Inc., Hackensack, NJ) having a large field of view. Immediately after imaging at 24 h, the mice were killed and the biodistribution of the radiolabel was determined.

The study was repeated using the same procedures, except that most of the urine was carefully removed with a syringe before imaging and only the imaging at 3 h was performed. Urine and plasma samples from mice killed at 3 h were analyzed by SE HPLC, the former by applying in-line radioactivity detection and the latter by collecting fractions for counting in a NaI(Tl) well counter.

RESULTS

Quality Assurance of Labeled cMORF

Figure 1 presents ultraviolet chromatograms of native cMORF and MAG3-coupled cMORF and the radiochromatogram of $^{99\text{m}}\text{Tc}$ -MAG3-cMORF. The labeling efficiency of labeled cMORF was between 40% and 60%. The radio-

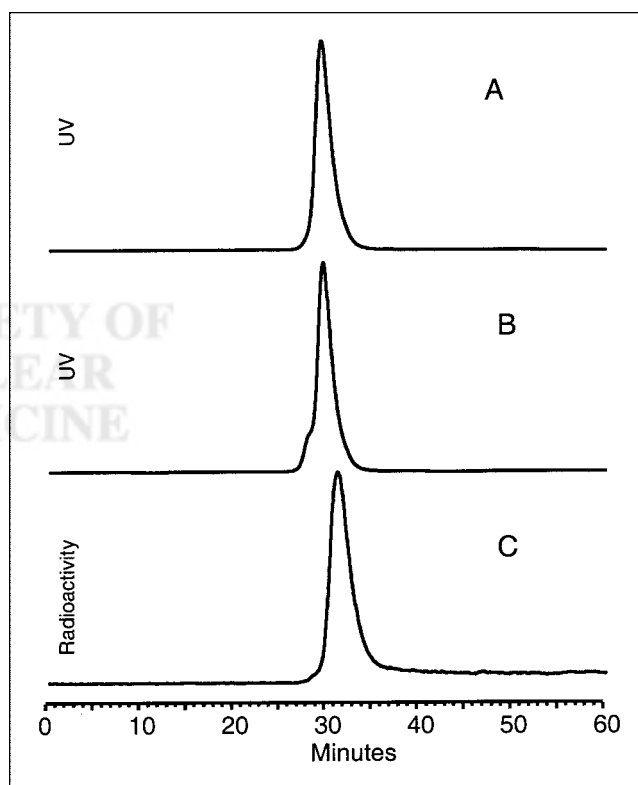


FIGURE 1. Ultraviolet (UV, 260 nm) SE HPLC profiles of uncoupled, native cMORF (A) and MAG3-coupled cMORF (B) and radioactivity profile of $^{99\text{m}}\text{Tc}$ -labeled MAG3-cMORF (C).

activity recovery of labeled cMORF off the HPLC was always >90%. The retention time of both native and coupled cMORF was 29.5 min; however, the latter showed a small shoulder with a retention time of approximately 28 min (possibly a result of MAG3-cMORF dimer formation through disulfide bonds). The radiolabeled cMORF showed a slightly longer retention time of 31.1 min.

Under the conditions of the bead study, $90.2\% \pm 0.9\%$ ($n = 3$) of the labeled cMORF bound to MORF beads, compared with only $0.4\% \pm 0.1\%$ and $0.3\% \pm 0.1\%$ ($n = 3$) of the labeled cMORF in the case of the blank control and the biotin-cMORF control, respectively. The radioactivity on beads in the study group was therefore caused by hybridization of labeled cMORF to MORF on the beads. These hybridization results of ^{99m}Tc -MAG3-cMORF (18mer) to MORF (18mer) on beads agree with earlier results from this laboratory on hybridization on beads of a ^{99m}Tc -MAG3-MORF (15mer) to cMORF (15mer) (30).

The single peak observed for labeled cMORF by HPLC (Fig. 1C) and the fact that at least 90% of the radioactivity hybridized to its complement in the bead study indicate that coupling with NHS-MAG3, purification on the P4 column,

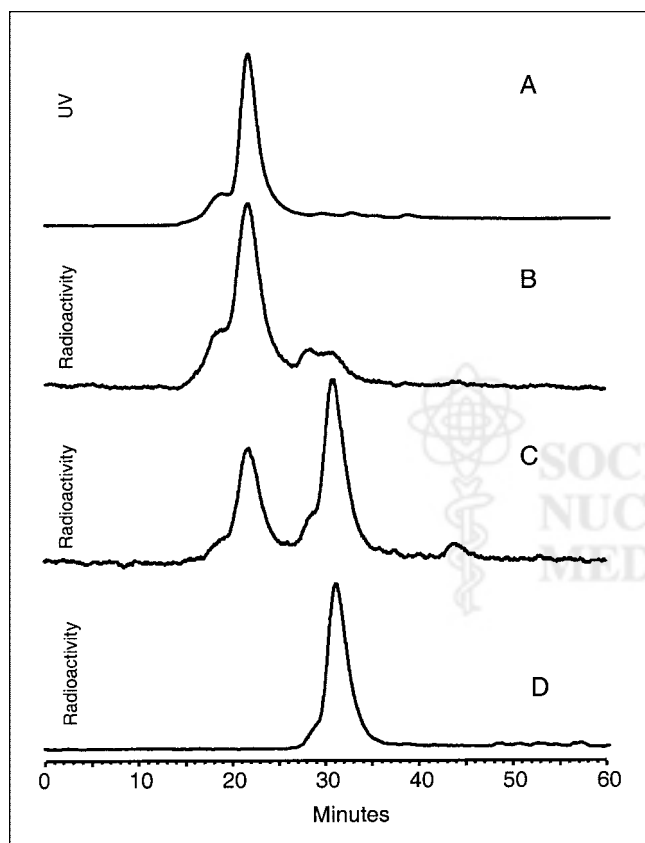


FIGURE 2. Ultraviolet (UV, 260 nm) SE HPLC profile of MN14-MORF (A), radioactivity profiles of labeled cMORF added to MN14-MORF at weight ratios of 0.04 $\mu\text{g}/25 \mu\text{g}$ (B) and 0.25 $\mu\text{g}/25 \mu\text{g}$ (C), and radioactivity profile of labeled cMORF added to native MN14 as control (D). Extent of labeled cMORF binding decreased as weight of labeled cMORF increased.

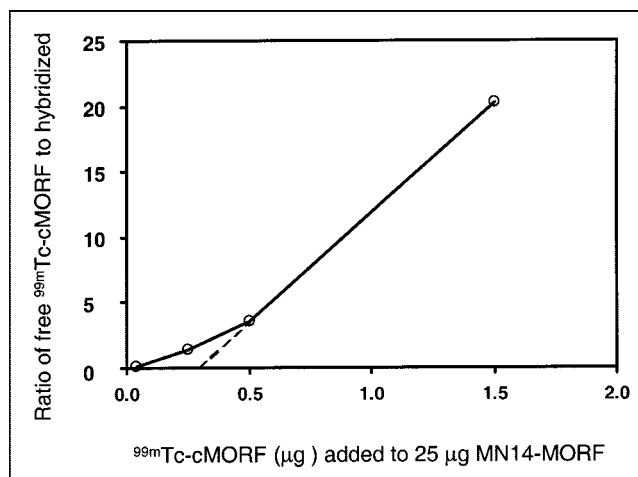


FIGURE 3. Plot of data from saturation study shows variation in ratio of free labeled cMORF to labeled cMORF-MN14-MORF as increasing weights of labeled cMORF were added. Curve was extrapolated to origin to estimate average number of MORF groups per MN14 molecule.

labeling with ^{99m}Tc , and purification again on the P4 column provided a satisfactory radiolabeled cMORF.

Estimation of MORF Groups per Molecule on Coupled MN14

Figure 2 presents HPLC profiles obtained by the hybridization of MN14-conjugated MORF with labeled cMORF. Recovery of radioactivity was >90%. The ultraviolet chromatogram of MN14-MORF is presented for reference (Fig. 2A), along with the radioactivity profile of a mixture of 50 μL (25 μg) native MN14 and 4 μL (0.04 μg) labeled cMORF (Fig. 2D). When the same weight of labeled cMORF was added to the same weight of MN14-MORF instead of native MN14, a shift of at least 80% to a higher molecular weight was evident (Fig. 2B). The 20% remaining was composed of 2 peaks, one with a retention time corresponding to labeled cMORF and another with the same retention time as a hybridized duplex of MORF and labeled cMORF (data not presented). Thus, the 2 peaks were probably caused by, respectively, traces of free labeled cMORF and labeled cMORF hybridized to free MORF not removed during purification of the MN14 preparation. That 80% of labeled cMORF bound to MN14 shows that MORF was coupled successfully to the antibody and was still capable of hybridizing. Native MN14 did not bind ^{99m}Tc -MAG3-cMORF (Fig. 2D).

Figure 2 also presents radiochromatograms of a mixture of 25 μL (0.25 μg) labeled cMORF and 50 μL (25 μg) MN14-MORF (Fig. 2C). More than half of the radioactivity is not hybridized under these conditions. Increasing the dosage of labeled cMORF to 50 μL or 150 μL increases the relative size of the peak of free ^{99m}Tc -MAG3-cMORF as the MORF molecules on MN14 become saturated. Results from this saturation study have been used to estimate the average number of MORF groups on MN14, as shown in Figure 3.

TABLE 1
Biodistribution of ^{99m}Tc-cMORF in 4 Healthy Mice

Site	0.5 h		1.0 h		3.0 h	
	Mean	SD	Mean	SD	Mean	SD
Organ (%ID/g)						
Liver	0.23	0.06	0.15	0.02	0.15	0.04
Heart	0.22	0.07	0.07	0.01	0.04	0.01
Kidneys	6.10	0.75	7.10	0.57	6.40	1.02
Lungs	0.42	0.09	0.15	0.02	0.07	0.01
Spleen	0.16	0.02	0.10	0.02	0.09	0.02
Muscle	0.17	0.04	0.09	0.07	0.02	0.01
Blood	0.74	0.18	0.18	0.05	0.04	0.01
Whole body (%ID)	22.50	4.40	11.70	2.30	7.00	1.00

%ID = percentage injected dose.

This figure is a plot of the ratio of free labeled cMORF to labeled cMORF bound to MN14-MORF as a function of labeled cMORF added. From the extrapolation of the straight region of the curve, the average number of MORF groups per MN14 was estimated to be 0.27. This method of estimating groups per molecule was subsequently confirmed by analyzing a nearly identical sample using a more accurate method based on HPLC analysis with dual ultraviolet absorbance detection. The result, at 0.28, agreed closely.

Biodistribution in Mice

Table 1 lists the biodistribution results of ^{99m}Tc in normal CD-1 mice at 0.5, 1, and 3 h after injection of ^{99m}Tc-cMORF. The whole-body radioactivity, in percentage injected dose (%ID), remaining at these times (not including urine) was 23, 12, and 7, respectively. No significant uptake occurred in the liver, small intestines, and large intestines, indicating that the labeled cMORF was almost solely excreted through the kidneys. The highest radioactivity levels, at 6–7 %ID/g throughout, were in the kidneys. At 0.5 h, the blood level (0.7 %ID/g) was relatively high, but at 1 h, the blood and all other organs except the kidneys were <0.2 %ID/g.

In Table 2, the biodistribution data for tumor-bearing nude mice show that, with the exception of the kidneys, radioactivity accumulated primarily in tumor, with values of 1.7–1.8 %ID/g, and that the radiolabel was retained in tumor over 24 h. Whole-body radioactivity levels for the study animals were 14 and 11 %ID at 3 and 24 h, respectively, whereas these values for the control animals were 7 and 5 %ID, respectively (in all cases with urine removed).

Figure 4 presents HPLC radiochromatograms of urine at 3 h obtained from a control animal and from a study animal. These results suggest that radioactivity in urine was present as intact labeled cMORF (Fig. 1C) and, therefore, that labeled cMORF is stable *in vivo*.

Figure 4 also presents radiochromatograms of plasma from a control animal and a study animal at 3 h. Because radioactivity levels were too low for measurement by the in-line radioactivity detector, fractions off the HPLC were collected for counting in a well NaI(Tl) detector. In the figure, the axes have been adjusted so that retention times for all panels may be compared. There is no radioactive peak in plasma from the control animal (Fig. 4C), whereas the radiochromatogram of plasma on the same scale from the study animal (Fig. 4D) shows only 1 radioactive peak, corresponding in retention time to labeled cMORF hybridized to MN14-MORF (Fig. 2B). The higher blood radioactivity in the study animals than in the control animals (Table 2) indicates that a considerable amount of the radiolabeled antibody was still in circulation in the study animals after 48 h, at the time when the labeled cMORF was injected (as expected for an IgG antibody). In the absence of the antibody, the labeled cMORF cleared rapidly, as shown in the control animals.

Imaging Study of LS174T Tumor-Bearing Nude Mice

Figure 5 presents whole-body images at 3 and 24 h after injection of labeled cMORF in the tumor-bearing mice previously injected with MN14-MORF 48 h earlier. The tumor is clearly seen in the study animals, in contrast to the control animals not receiving MN14-MORF. In one early image (Fig. 5A), radioactivity in the bladder is pronounced

TABLE 2
Biodistribution of ^{99m}Tc-cMORF in 4 LS174T Tumor-Bearing Nude Mice

Site	3 h				24 h			
	Control		Study		Control		Study	
	Mean	SD	Mean	SD	Mean	SD	Mean	SD
Organ (%ID/g)								
Liver	0.23	0.01	0.41	0.05	0.10	0.01	0.60	0.05
Heart	0.04	0.01	0.18	0.01	0.02	0.00	0.13	0.02
Kidneys	6.40	1.95	6.90	1.96	3.20	0.68	4.00	1.00
Lungs	0.07	0.01	0.34	0.06	0.04	0.01	0.24	0.04
Spleen	0.11	0.01	0.29	0.08	0.07	0.01	0.31	0.04
Muscle	0.03	0.03	0.09	0.01	0.02	0.00	0.07	0.01
Tumor	0.09	0.01	1.80	0.24	0.05	0.00	1.70	0.14
Blood	0.04	0.01	1.02	0.13	0.00	0.01	0.50	0.12
Whole body (%ID)	6.90	3.30	14.40	0.90	5.00	2.00	11.40	0.70

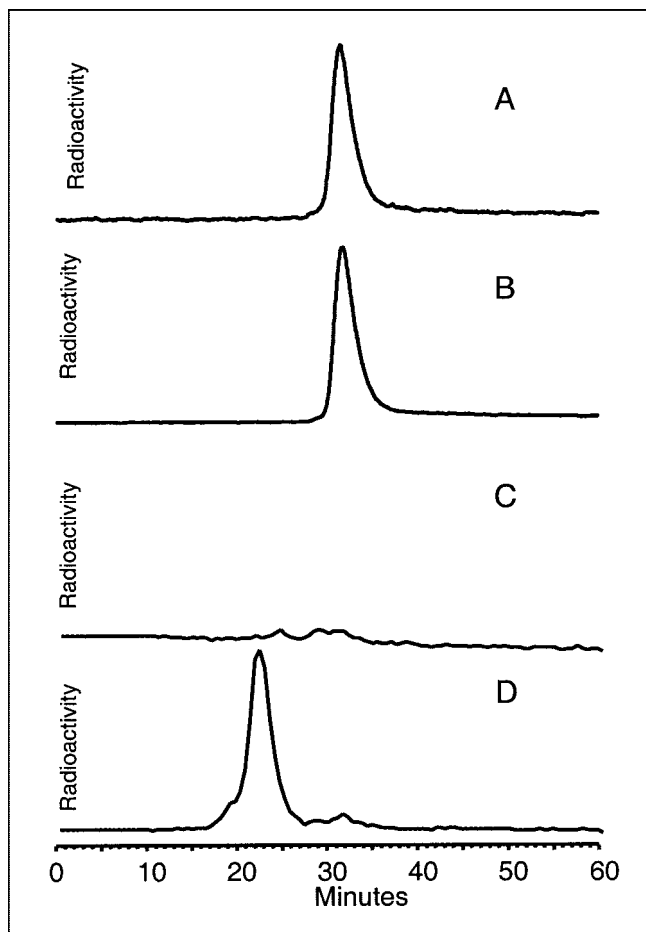


FIGURE 4. Radioactivity SE HPLC profiles of urine obtained at 3 h from control mouse receiving only labeled cMORF (A) and from study mouse receiving both MN14-MORF and labeled cMORF (B) and radiochromatograms, on same axes, of plasma obtained at 3 h from control mouse (C) and from study mouse (D). Results show that radioactivity in urine was present primarily as labeled cMORF, whereas in plasma, significant levels of radioactivity were present only in study mice and then only as labeled cMORF-MN14-MORF.

and at interfering levels. At 24 h (Fig. 5C), however, urine activity diminished, so that the image clearly shows only the tumor and kidneys. On the image obtained after removal of the urine (Fig. 5B), only the kidneys and tumor are prom-

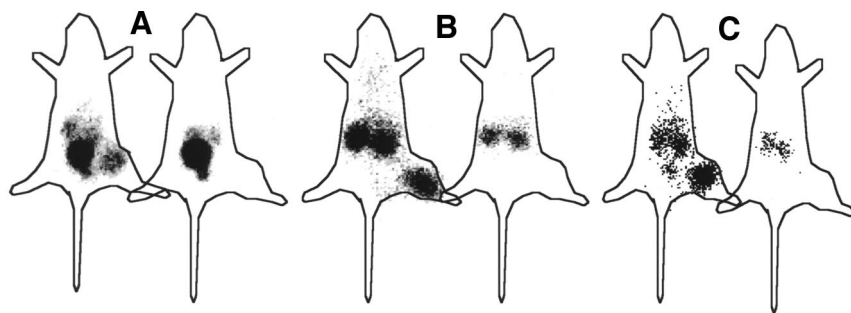


FIGURE 5. Gamma camera images of LS174T tumor-bearing nude mice show whole-body anterior views obtained at 3 h (A) and 24 h (C) and, during repeated study after removal of urine, at 3 h (B). In each pair of images, study animal is on left and control animal is on right.

inent. In all 3 images, the tumor is not visible in the control animals.

DISCUSSION

To be useful for radiopharmaceutical applications including pretargeting, radiolabeled MORFs must hybridize effectively *in vivo* and must also clear rapidly, preferably through the kidneys. Both properties were evident in this investigation of an 18mer MORF conjugated with NHS-MAG3 and radiolabeled with ^{99m}Tc .

As concerns *in vitro* hybridization, we showed earlier (30) by surface plasmon resonance that the association rate constant of MORF is unchanged by MAG3 conjugation and is comparable with that of native and conjugated DNAs and PNAs. In that investigation, we were also able to show >85% stability of the ^{99m}Tc on MAG3-MORF over 24 h in 37°C serum with minimal protein binding. Finally, we were able to target labeled MORF to cMORF beads in the thigh of normal mice (30). In the current investigation, we have again shown hybridization *in vitro*—this time, of labeled cMORF to MORF. More important to pretargeting applications, hybridization of labeled cMORF to MORF-conjugated MN14 has also now been shown *in vitro* by HPLC (Fig. 2).

With regard to the pharmacokinetic properties of labeled cMORF, in our earlier investigation we observed rapid clearance of ^{99m}Tc -MAG3-MORF in normal mice, with only 21% of the radiolabel remaining after 3 h (30). Even though representing rapid clearance, this whole-body value was higher than the 7% reported here (Table 1). The discrepancy is related less to any differences in pharmacokinetics between labeled MORF and cMORF, or to the small differences in dosages administered (0.3 vs. 1.5 μg), than to the removal of urine in this current study. Nevertheless, by all measures, the pharmacokinetics of radiolabeled MORFs are rapid. Furthermore, in at least the case of the 18mer-labeled cMORF, clearance was almost exclusively through the kidneys and as intact labeled cMORF (Fig. 4).

This laboratory has long had an interest in pretargeting, initially using streptavidin (or avidin) and biotin and more recently using oligomers such as DNAs and PNAs (11,20,26,34–38). A meaningful comparison of tumor pretargeting among the results from this laboratory is made

difficult by nonuniform experimental designs. Nevertheless, in a comparison of streptavidin and ^{99m}Tc -biotin, PNA-streptavidin and ^{99m}Tc -cPNA, and MN14-MORF and ^{99m}Tc -cMORF, much higher dosages were used in the PNA study to provide relatively low tumor uptake (0.3 %ID/g) and a poor tumor-to-blood ratio (0.4) (26). Although the results in the use of streptavidin and biotin (35) and of MN14-MORF and labeled cMORF were similar (tumor uptake of 1.8%ID/g at 2–3 h, tumor-to-blood ratios of 1.8–2.2), the former relied on nonspecific diffusion of streptavidin into tumors whereas the current investigation had the advantage of specific tumor targeting through an anti-CEA antibody.

More meaningful may be a comparison between conventional tumor targeting and pretargeting. The murine IgG antibody MN14 has been labeled with radioiodine and studied in tumor-bearing mice (39,40). Approximately 3 h after administration of 2 μg labeled antibody, tumor uptake was approximately 5 %ID/g and therefore somewhat higher than that observed in the current study. However, at the same time, the tumor-to-blood ratio was approximately 0.5 and the ratios of tumor to other tissues were also relatively poor. These results show that even though absolute tumor uptake may be lower in pretargeted imaging than in conventional imaging, pretargeting has the potential for achieving earlier and better ratios of tumor to normal tissues.

Unlike most pretargeting studies, this investigation did not include a clearance step. As shown in Figure 4D, antibody was still circulating at 48 h and capable of binding the labeled cMORF. The result was higher blood radioactivity levels and lower ratios of tumor radioactivity to normal-tissue radioactivity; however, the expected improvement in imaging by including a clearing step may not justify the added complexity, because at 3 h only 1 %ID/g of the radiolabel was in blood (Table 1). Use of a clearing agent may be more important to therapy studies. Finally, one would also expect the results to have improved using an MN14 with a higher average number of MORFs than 0.3.

CONCLUSION

When radiolabeled with ^{99m}Tc through MAG3, an 18mer cMORF displayed label stability, hybridization ability, and rapid pharmacokinetics. When the cMORF was used along with an antitumor antibody conjugated with MORF, pretargeting was achieved in tumor-bearing mice. The biodistribution shown by imaging the animals revealed low radioactivity levels in all tissues other than the kidneys, even as early as 3 h after administration, and good radioactivity levels in tumor. Our results suggest that morpholinos should be considered further for pretargeting and for other nuclear medicine imaging applications.

ACKNOWLEDGMENTS

The authors are grateful to Drs. James Summerton and Paul Morcos of GeneTools for providing the morpholinos and to Dr. Gary Griffiths of Immunomedics for providing

the MN14. This study was supported in part by grant CA79507 from the National Institutes of Health.

REFERENCES

1. Goldenberg DM, Deland F, Kim E, et al. Use of radiolabeled antibodies to carcinoembryonic antigen for detection and localization of diverse cancers by external photoscanning. *N Engl J Med*. 1978;298:1384–1386.
2. Goldenberg DM, Juweid M, Dunn RM, Sharkey RM. Cancer imaging with radiolabeled antibodies: new advances with technetium-99m-labeled monoclonal antibody Fab' fragments, especially CEA-Scan and prospects for therapy. *J Nucl Med Technol*. 1997;25:18–23.
3. Lister-James J, Moyer BR, Dean RT. Pharmacokinetic considerations in the development of peptide-based imaging agents. *Q J Nucl Med*. 1997;41:111–118.
4. Lister-James J, Moyer BR, Dean RT. Small peptides radiolabeled with ^{99m}Tc . *Q J Nucl Med*. 1996;40:221–233.
5. Goodwin DA, Meares CF. Pretargeting: general principles. *Cancer*. 1997;80(suppl):2675s–2680s.
6. Goodwin DA. Tumor pretargeting: almost the bottom line. *J Nucl Med*. 1995;36:876–879.
7. Stoldt HS, Aftab F, Chinol M, et al. Pretargeting strategies for radio-immunoguided tumour localization and therapy. *Eur J Cancer*. 1997;33:186–192.
8. Sakahara H, Saga T. Avidin-biotin system for delivery of diagnostic agents. *Adv Drug Deliv Rev*. 1999;37:89–101.
9. Wilbur DS, Pathare PM, Hamlin DK, et al. Development of new biotin/streptavidin reagents for pretargeting. *Biomol Eng*. 1999;16:113–118.
10. Barbet J, Kraeber-Bodere F, Vuillez JP, et al. Pretargeting with the affinity enhancement system for radioimmunotherapy. *Cancer Biother Radiopharm*. 1999;14:153–166.
11. Hnatowich DJ, Virzi F, Rusckowski M. Investigations of avidin and biotin for imaging applications. *J Nucl Med*. 1987;28:1294–1302.
12. Goodwin DA, Meares CF, McTigue M, et al. Rapid localization of haptens in sites containing previously administered antibody for immunoscintigraphy with short half-life tracers [abstract]. *J Nucl Med*. 1986;27(suppl):959.
13. Kuijpers WH, Bos ES, Kaspersen FM, Veeneman GH, van Boeckel CA. Specific recognition of antibody-oligonucleotide conjugates by radiolabeled antisense nucleotides: a novel approach for two-step radioimmunotherapy of cancer. *Bioconjug Chem*. 1993;4:94–102.
14. Knox SJ, Goris ML, Tempero M, et al. Phase II trial of yttrium-90-DOTA-biotin pretargeted by NR-LU-10 antibody/streptavidin in patients with metastatic colon cancer. *Clin Cancer Res*. 2000;6:406–414.
15. Cremonesi M, Ferrari M, Chinol M, et al. Three-step radioimmunotherapy with yttrium-90 biotin: dosimetry and pharmacokinetics in cancer patients. *Eur J Nucl Med*. 1999;26:110–120.
16. Goshorn S, Sanderson J, Axworthy D, Lin Y, Hylarides M, Schultz J. Preclinical evaluation of a humanized NR-LU-10 antibody-streptavidin fusion protein for pretargeted cancer therapy. *Cancer Biother Radiopharm*. 2001;16:109–123.
17. Rosebrough SF. Plasma stability and pharmacokinetics of radiolabeled deferoxamine-biotin derivatives. *J Pharmacol Exp Ther*. 1993;265:408–415.
18. Paganelli G, Malcoviti M, Fazio F. Monoclonal antibody pretargeting techniques for tumor localization: the avidin-biotin system. *Nucl Med Commun*. 1991;12:211–234.
19. Sharkey RM, Karacay H, Griffiths GL, et al. Development of a streptavidin-anti-carcinoembryonic antigen antibody, radiolabeled biotin pretargeting method for radioimmunotherapy of colorectal cancer: studies in a human colon cancer xenograft model. *Bioconjug Chem*. 1997;8:595–604.
20. Rusckowski M, Fogarasi M, Fritz B, Hnatowich DJ. Effect of endogenous biotin on the applications of streptavidin and biotin in mice. *Nucl Med Biol*. 1997;24:263–268.
21. Karacay H, McBride WJ, Griffiths GL, et al. Experimental pretargeting studies of cancer with a humanized anti-CEA x murine anti-[In-DTPA] bispecific antibody construct and a (^{99m}Tc)-(188)Re-labeled peptide. *Bioconjug Chem*. 2000;11:842–854.
22. Gautherot E, Rouvier E, Daniel L, et al. Pretargeted radioimmunotherapy of human colorectal xenografts with bispecific antibody and ^{131}I -labeled bivalent hapten. *J Nucl Med*. 2000;41:480–487.
23. Lubic SP, Goodwin DA, Meares CF, Song C, Osen M, Hays M. Biodistribution and dosimetry of pretargeted monoclonal antibody 2D12.5 and Y-Janus-DOTA in BALB/c mice with KHJJ mouse adenocarcinoma. *J Nucl Med*. 2001;42:670–678.
24. Gestin JF, Loussouarn A, Bardies M, et al. Two-step targeting of xenografted colon carcinoma using a bispecific antibody and ^{188}Re -labeled bivalent hapten: biodistribution and dosimetry studies. *J Nucl Med*. 2001;42:146–153.

25. Zhu H, Jain RK, Baxter LT. Tumor pretargeting for radioimmunodetection and radioimmunotherapy. *J Nucl Med.* 1998;39:65–76.
26. Rusckowski M, Qu T, Chang F, Hnatowich DJ. Pretargeting using peptide nucleic acid. *Cancer.* 1997;80:2699–2705.
27. Bos ES, Kuijpers WH, Meesters-Winters M, et al. In vitro evaluation of DNA-DNA hybridization as a two-step approach in radioimmunotherapy of cancer. *Cancer Res.* 1994;54:3479–3486.
28. Hnatowich DJ. Pharmacokinetic considerations in the development of oligomers as radiopharmaceuticals. *Q J Nucl Med.* 1997;41:91–100.
29. Summerton J, Weller D. Morpholino antisense oligomers: design, preparation, and properties. *Antisense Nucleic Acid Drug Dev.* 1997;7:187–195.
30. Mang'era KO, Liu G, Wang Y, et al. Initial investigation of ^{99m}Tc-labeled morpholinos for radiopharmaceutical applications. *Eur J Nucl Med.* 2001;28:1682–1689.
31. Wang Y, Chang F, Zhang Y, et al. Pretargeting with amplification using polymeric peptide nucleic acid (PNA). *Bioconjug Chem.* 2001;12:807–816.
32. Winnard P Jr, Chang F, Rusckowski M, Mardirossian G, Hnatowich DJ. Preparation and use of NHS-MAG₃ for technetium-99m labeling of DNA. *Nucl Med Biol.* 1997;24:425–432.
33. Mardirossian G, Lei K, Rusckowski M, et al. In vivo hybridization of technetium-99m-labeled peptide nucleic acid (PNA). *J Nucl Med.* 1997;38:907–913.
34. Kalofonos HP, Rusckowski M, Siebecker DA, et al. Radioimmunotargeting of tumor in patients with streptavidin and biotin: preliminary communication. *J Nucl Med.* 1990;31:1791–1796.
35. Hnatowich DJ, Fritz B, Virzi F, Mardirossian G, Rusckowski M. Improved tumor localization with (strept)avidin and labeled biotin as a substitute for antibody. *Nucl Med Biol.* 1993;20:189–193.
36. Rusckowski M, Fritz B, Hnatowich DJ. Localization of infection using streptavidin and biotin: an alternative to nonspecific polyclonal IgG. *J Nucl Med.* 1992;33:1810–1815.
37. Rusckowski M, Fogarasi M, Fritz B, Hnatowich DJ. Influence of endogenous biotin on the biodistribution of two In-111 labeled biotin derivatives in mice. *Nucl Med Commun.* 1995;16:38–46.
38. Fogarasi M, Pullman J, Winnard P Jr, Virzi F, Hnatowich DJ, Rusckowski M. Pretargeting of bacterial endocarditis in rats with streptavidin and ¹¹¹In-biotin. *J Nucl Med.* 1999;40:484–490.
39. Hansen HJ, Goldenberg DM, Newman ES, Grebenau R, Sharkey RM. Characterization of second-generation monoclonal antibodies against carcinoembryonic antigen. *Cancer.* 1993;71:3478–3485.
40. Sharkey RM, Juweid M, Shevitz J, et al. Evaluation of a complementarity-determining region-grafted (humanized) anti-carcinoembryonic antigen monoclonal antibody in preclinical and clinical studies. *Cancer Res.* 1995;55(suppl):5935s–5945s.

